EasyChair Preprint

№ 900

Passive radar using Starlink transmissions: A theoretical study

Alp Sayin, Mikhail Cherniakov and Michail Antoniou

April 14, 2019

Passive radar using Starlink transmissions: A theoretical study

Alp Sayin, Mikhail Cherniakov, Michail Antoniou
Department of Electronic, Electrical and Systems Engineering, University of Birmingham
Birmingham, UNITED KINGDOM
email: m.antoniou@bham.ac.uk

Abstract: *SpaceX plans to build two NGSO constellations, named Starlink, to provide high speed internet to end-users. The system will have global coverage 24/7 by means of launching 4425 satellites on circular low orbits. In this paper, the possibility of using these satellite emissions as an illuminating source for bistatic real and synthetic aperture radars, assuming a receiver on or near the earth surface, is investigated. The practicality of these systems are discussed for possible applications.*

1. Introduction

Passive radar systems with spaceborne illuminators of opportunity are desirable for numerous reasons, including their unique potential for persistent surveillance/remote sensing and, more importantly, operation anywhere on Earth, compared to terrestrial transmitters. Typically, communication or navigation satellites are used for this purpose, however different systems have their own, varying limitations from a radar point of view which restrict their field of application. For example, Global Navigation Satellite Systems (GNSS) have a global and persistent coverage, but a very restricted power budget [1]. Communication satellites, such as Inmarsat or Iridium, have a better power budget but their transmitted signals offer a poor range resolution [2] and may (Iridium) or may not do not have a global coverage. Broadcasting satellites in geostationary orbits, such as DVB-S, can have a high spatial resolution [3] but a modest power budget and do not have a global coverage by default, in addition to Northern Hemisphere being only illuminated from South which restricts potential observation capability.

Recently, a new kind of spaceborne transmitter has been brought forward- satellites for broadband internet services. SpaceX Exploration Technologies Corp. has revealed its plans to build two non-geostationary orbit (NGSO) constellations of thousands of satellites, called Starlink to provide internet to end-users and gateways operating at X- and V- bands, with the aim of having global coverage at all times at least via one satellite. Apart from global and persistent coverage, the unique opportunity these new satellites provide is that they can offer very wide transmit signal bandwidths (quoted up to 1 Gbps), which can provide fine range resolutions, but also a substantial amount of energy spread across these bandwidths, which is critical for their power budget. Other players like OneWeb are also working on their own constellations with similar technical characteristics and similar goals [4], [5]. For this reason we will concentrate on Starlink in this paper for brevity, but without loss of generality.

In parallel, the field of broadband satellite internet is progressing at a rapid pace and this can be seen by numerous activities. OneWeb has scheduled test launches for the first quarter of 2019. Numerous patent applications on the Starlink satellites and their antennas have already been filed or granted [6]. In addition, in November 2018 the US Federal Communications Commission (FCC) granted approval for over 7,000 Starlink satellites to be launched [7], [8]. Crucially, in February 2018 two Starlink test satellites (Tintin A&B) were launched alongside the PAZ (“peace” in Spanish) radar satellite.

Therefore, it appears a satellite internet system may well become reality in the future, and current technical characteristics, which seem similar across different constellations, can be used as a basis for estimating radar performance for detection and/or imaging, which is the subject

of this paper. The methodology of the analysis used by the authors is the same as have been used for GNSS based passive radar where all the analytical study results are well experimentally verified in a number of authors' previous work [9]–[14]. The emphasis is placed on power budget and detection range, which forms the backbone of any radar system.

The paper is organised as follows: Section 2 conveys relevant specification information from the officially released Starlink documents such as FCC and patent applications, which form the basis for radar performance calculations. Section 3 presents power budget calculations for detection, and discusses the feasibility of the proposed system. The results are compared to those of a GNSS-based radar as a basis for comparison. Since this is a paper abstract, this version of the paper summarises major methods and results. The full analyses will be shown at the full version of the paper.

2. Satellite parameters

From [7], it is believed that Starlink will create the equivalent of a surface cellular structure similar to mobile telephony networks, with satellite antenna beams replacing terrestrial cellular towers. This is to be achieved by Starlink's phased array antennas, which can steer multiple narrow beams electronically. Based on the same documentation, the constellation will operate on the basis that a cell is only illuminated with a single beam (single frequency band) at any given time, regardless of the number of satellites available to give coverage to that cell. The area a single satellite can cover is conditionally shown in Figure 1a, with the intended cell structure provided by a single satellite in Figure 1b [7].

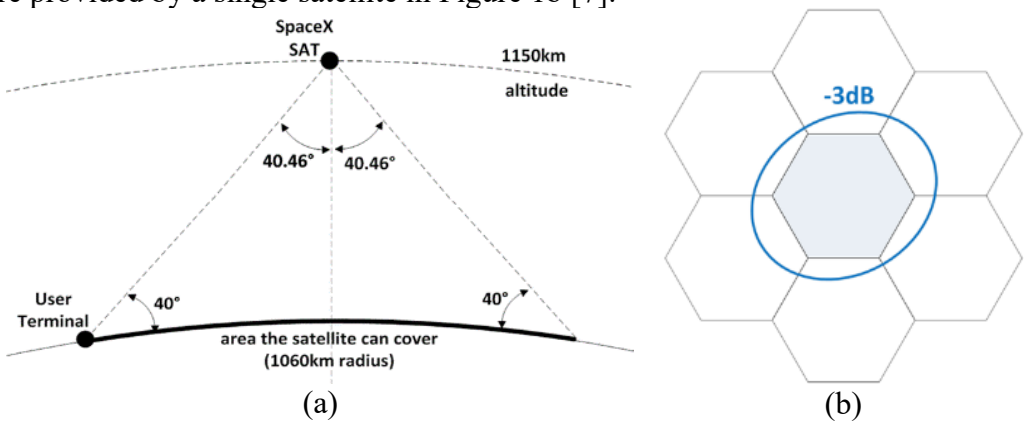

Figure 1. (a) Coverage area summary, (b) Intended beam coverage area

A single cell is defined by the transmitter azimuth and elevation beamwidths. Using a custom-design phased array, the 3dB-beamwidth is kept under 2.5^0 per beam with variations between 2.15^0 minimum to 2.45^0 maximum. This is to be achieved by switching on additional phased array elements as the steering angle increases. In addition to that, beam contours at nadir can be seen in Figure 2 [7]. Contours are given at -2, -4, -6, -10, -15 and -20 dB. Using a 2.5^0 beamwidth at elevation and at azimuth at nadir (1110 km) would yield a spot beam whose footprint would have a diameter of about 48 km at that distance. For the sake of simplicity, it is assumed that proposed system operates within a single cell.

In terms of transmitting signals, it is proposed to use a downlink signal. The downlink signal itself is 2 GHz wide and at X-band, from 10.7 to 12.7 GHz. However, if a terrestrial cellular network structure is to be replicated, we may assume that different cells from a single satellite will use a portion of that bandwidth. Satellites will create 7 beams as in Figure 1b, and each one is allocated equal bandwidths (nearly 250 MHz in each cell according to published documents), which yields a quasi-monostatic range resolution of approximately 0.6m.

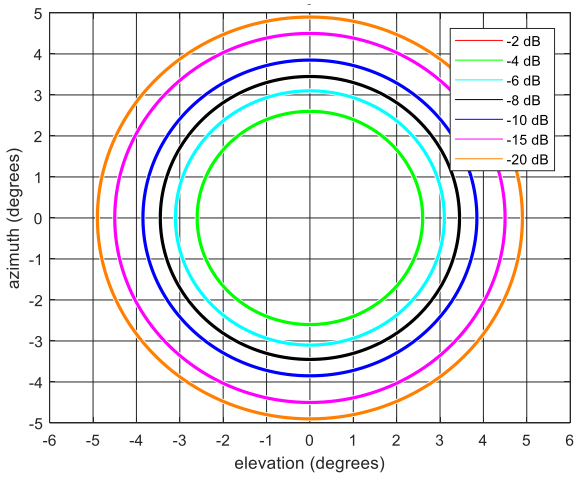

Figure 2. Transmit beam contours at various scanning angles at nadir

SpaceX's FCC application suggests their arrays will be forming beams with different frequencies, and the documents do not mention beamforming capabilities with a combined bandwidth [15, p. 247]. Therefore, it's inferred that multiplexing will be done via FDMA only. If there's at least one active -broadband- user during measurements within the same cell as target, this already ensures target is illuminated. We can further assume that even if the human users may not be active, modems will be. We expect that modems will be actively engaging with satellites for session and network management and similar tasks. The intensity of these activities may be less than an active user, however the probability of having non-interleaved transmissions then would increase with respect to number of subscribers. Finally, since there is only one user needed for illumination, theoretically the constellation could be "tricked" into illuminating a target by asking for service, but this is not in the scope of this study.

3. Power budget estimation

In this section, the power budget for detection is calculated. The analysis is similar to previous work done on GNSS-based radar [1]. In addition, results obtained from Starlink are compared to those of GNSS-based system to gain an appreciation of relative merits and drawbacks.

3.1 Passive Radar Parameters

Returns from a single satellite cell, over a 250MHz bandwidth is assumed. For the sake of simplicity, the size of both the reference antenna (for direct signal reception) and the radar antenna (for echo reception) is assumed to be 1 m^2, however antenna surface area could also be included as a design parameter. At X-band, the beamwidth of such an antenna would be about 1.3 degrees. This antenna may be a phased array, or a multi-beam staring array for a chosen target area, but such design considerations are outside the scope of this manuscript. The remaining radar parameters for a Starlink-based and an equivalent GNSS-based radar system, can be seen in Table 1.

Table 1. Power budget calculation parameters for SpaceX and GNSS

Notation	*Parameter*	*GNSS*	*SpaceX*
F_c	Centre Frequency	1.1765 GHz	11.575 GHz
BW	Bandwidth	10.23 MHz	250 MHz
h_{rx}	Radar antenna height	1.5 m	1.5 m
A_{rx}	Antenna Effective Area	1 m^2	1 m^2
θ_{rx}	Antenna beamwidth	13 degrees	1.3 degrees
G_{rx}	Antenna gain	22.9 dB	42.7 dB
T_n	Noise temperature	300 K	300 K
P_n	Ambient Noise	-132.0 dB	-118.4 dB
N_f	Receiver Noise figure	1.4 dB	1.4 dB
L	System losses	6 dB	6 dB
σ	Target RCS	10 m^2	10 m^2
Δ_{range}	Range resolution	14.7m	0.6m

3.2 SNR at reference antenna output

The EIRP (effective isotropic radiation power) at the Starlink antenna output and the Power Flux Density (PFD) near the ground can be found below in Table 2 [7]. The table shows that the transmit antenna array adjusts output power to ensure a PFD of -182 dBW/m^2/Hz compared to -203.8 dBW/m^2/Hz from its GNSS counterpart.

Table 2. EIRP and PFD values

Notation	*Parameter*	*Starlink at Slant*	*Starlink at Nadir*	*GNSS*
EIRP	Equivalent Isotropically Radiated Power at Satellite (dBW/Hz)	-47.1	-50.13	-46.68
R_{orbit}	Distance to Earth (km)	1574.58	1110.00	20200
FSPL	Spreading loss (dB)	-134.94	-131.90	-157.1
PFD	Power Flux Density at Ground (dB(W/m^2/Hz))	-182.02	-182.02	-203.8

Using the aforementioned parameters, the SNR at the reference antenna output can be calculated as:

$$\mathrm{SNR_{ref}} = \frac{\mathrm{EIRP} * BW}{4\pi R_{orbit}^2} * \frac{A_{rx}}{P_n} \tag{1}$$

Based on the parameters set in Table 1 and Table 2, the SNR at the output of the reference antenna is around 20 dB. This means that purely from a SNR point of view, the direct signal can be used as a reference signal for matched filtering directly as in most passive radar systems. However, for an antenna with a beamwidth of 1.3 degrees, a satellite tracking array may be needed over the available dwell time on target.

3.2 SNR

The SNR of a signal returned from two different target types, airborne and ground-based (or maritime) is calculated. The assumption for airborne targets is free-space propagation and for ground-based targets it is two-ray path (where multipath and clutter would also be present but are not considered in these first proof of concept calculations). The SNR at the output of a matched filter and an integration time of 1s is shown in Figure 3, based on the parameters of Table 2, for a hypothetical Starlink and GNSS-based radar. The figure assumes coherent (Co) and non-coherent (NC) integration, as well as the more pessimistic case (PC) which assumes that as the SNR for a single pulse goes below 0 dB, the signal processing gain from matched filtering will be deteriorated. The equations used in these calculations will be shown in the full version of the paper.

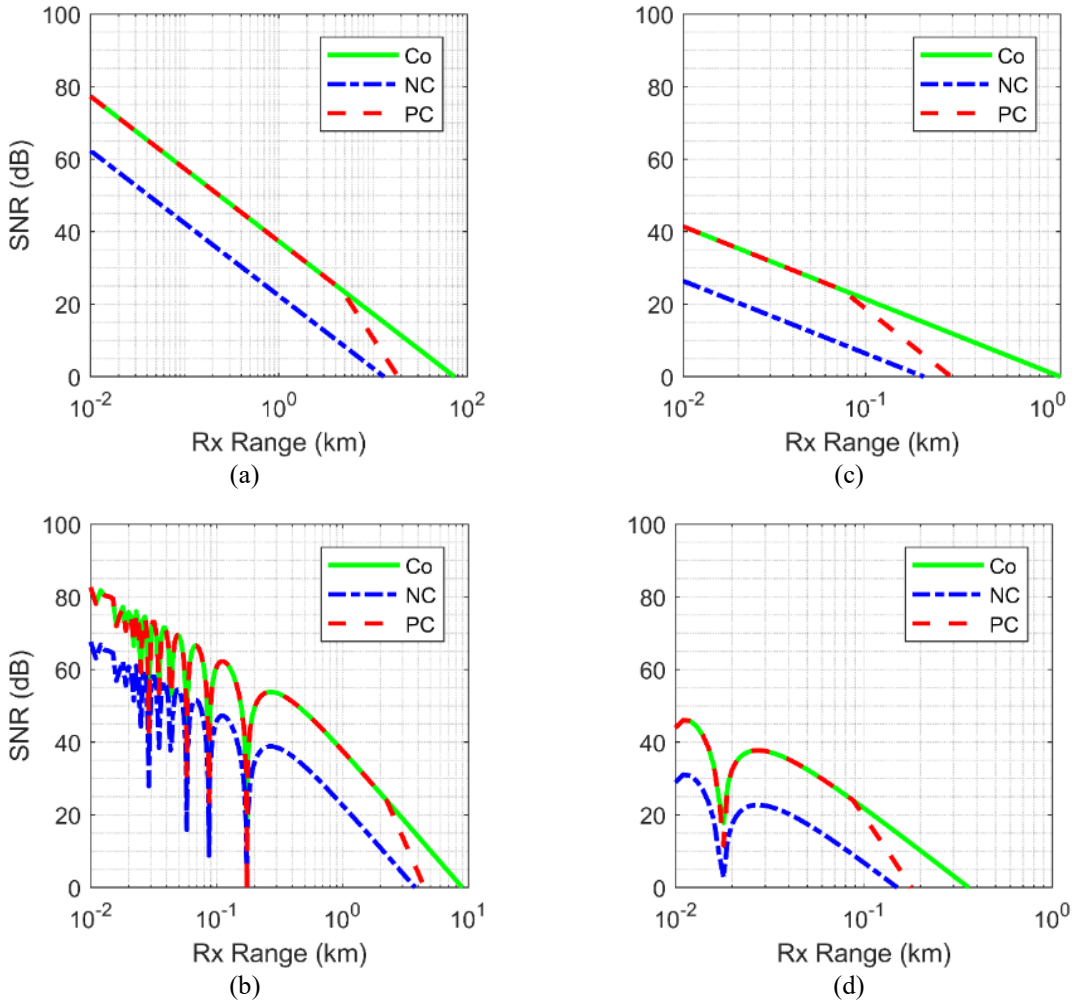

Figure 3 SNR after 1s integration (a) Starlink against airborne targets (b) Starlink against ground-targets (c) GNSS against airborne targets (d) GNSS against ground targets

The figure shows that setting a 12 dB SNR as the detection threshold, a coherent integration (best case) of 1s yields a maximum detection range for a $10m^2$ RCS airborne target of approximately 10km, while a purely non-coherent integration (worst case) brings this figure down to 2km. For a ground-based target where two-ray path propagation should be assumed, a target with the same RCS would be detected at a maximum range of approximately 4km for coherent and 1.5km for the worst case. An equivalent GNSS-based system would provide an equivalent 200m for the same airborne target, and approximately 10m for a ground-based target under best case conditions, which is two orders of magnitude less than Starlink.

4. Conclusions and Future Work

A study on passive radar detection capabilities using SpaceX broadband internet satellite constellation has been done and the system was found to be feasible when compared to an already proven system, GNSS, with a similar structure.

Future work will be concentrated on the structure of such a system, its applicability for SAR imaging, as well as proof-of-concept experiments with Starlink test satellites already in orbit.

5. References

[1] M. Antoniou and M. Cherniakov, 'GNSS-based passive radar', in *Real aperture array radar, imaging radar, and passive and multistatic radar*, Edison, NJ: SciTech Publishing, an imprint of the IET, 2017, pp. 719–766.

[2] Xiaoyong Lyu, S. Hristov, M. Gashinova, A. Stove, and M. Cherniakov, 'Ambiguity function analysis of the Inmarsat I-4 and Iridium signals', in *International Conference on Radar Systems (Radar 2017)*, Belfast, UK, 2017.

[3] I. Pisciottano, D. Cristallini, J. Schell, and V. Seidel, 'Passive ISAR for Maritime Target Imaging: Experimental Results', in *2018 19th International Radar Symposium (IRS)*, Bonn, Germany, 2018, pp. 1–10.

[4] FCC and Worldvu Satellites Limited as 'OneWeb', 'FCC Application Listing SATLOI2016042800041', *INTERNATIONAL BUREAU FCC SELECTED APPLICATION LISTING BY FILE NUMBER REPORT WR07*. [Online]. Available: https://licensing.fcc.gov/cgi-bin/ws.exe/prod/ib/forms/reports/swr031b.hts?q_set=V_SITE_ANTENNA_FREQ.file_numberC/File+Number/%3D/SATLOI2016042800041&prepare=&column=V_SITE_ANTENNA_FREQ.file_numberC/File+Number. [Accessed: 26-Oct-2018].

[5] FCC and Worldvu Satellites Limited as 'OneWeb', 'FCC Application Listing SATLOI2017030100031', *INTERNATIONAL BUREAU FCC SELECTED APPLICATION LISTING BY FILE NUMBER REPORT WR07*. [Online]. Available: https://licensing.fcc.gov/cgi-bin/ws.exe/prod/ib/forms/reports/swr031b.hts?q_set=V_SITE_ANTENNA_FREQ.file_numberC/File+Number/%3D/SATLOI2017030100031&prepare=&column=V_SITE_ANTENNA_FREQ.file_numberC/File+Number. [Accessed: 26-Oct-2018].

[6] S. Jalali Mazlouman, K. Schulze, and S. Sharma, 'Distributed Phase Shifter Array System and Method', WO/2018/152439, 24-Aug-2018.

[7] FCC and Space Exploration Holdings, 'FCC Application Listing SATLOA2016111500118', *INTERNATIONAL BUREAU FCC SELECTED APPLICATION LISTING BY FILE NUMBER REPORT WR07*, 15-Nov-2016. [Online]. Available: https://licensing.fcc.gov/cgi-bin/ws.exe/prod/ib/forms/reports/swr031b.hts?q_set=V_SITE_ANTENNA_FREQ.file_numberC/File+Number/%3D/SATLOA2017030100027&prepare=&column=V_SITE_ANTENNA_FREQ.file_numberC/File+Number. [Accessed: 11-Apr-2018].

[8] FCC and Space Exploration Holdings, 'FCC Application Listing SATLOA2017030100027', *INTERNATIONAL BUREAU FCC SELECTED APPLICATION LISTING BY FILE NUMBER REPORT WR07*, 01-Mar-2017. [Online]. Available: https://licensing.fcc.gov/cgi-bin/ws.exe/prod/ib/forms/reports/swr031b.hts?q_set=V_SITE_ANTENNA_FREQ.file_numberC/File+Number/%3D/SATLOA2016111500118&prepare=&column=V_SITE_ANTENNA_FREQ.file_numberC/File+Number. [Accessed: 11-Apr-2018].

[9] X. He, M. Cherniakov, and T. Zeng, 'Signal detectability in SS-BSAR with GNSS non-cooperative transmitter', *IEE Proceedings - Radar, Sonar and Navigation*, vol. 152, no. 3, p. 124, 2005.

[10] M. Antoniou, A. G. Stove, D. Tzagkas, M. Cherniakov, and H. Ma, 'Marine Target Localization with Passive GNSS-Based Multistatic Radar: Experimental Results', p. 5.

[11] H. Ma *et al.*, 'Maritime target detection using GNSS-based radar: Experimental proof of concept', in *2017 IEEE Radar Conference (RadarConf)*, Seattle, WA, USA, 2017, pp. 0464–0469.

[12] A. G. Stove, M. S. Gashinova, S. Hristov, and M. Cherniakov, 'Passive Maritime Surveillance Using Satellite Communication Signals', *IEEE Transactions on Aerospace and Electronic Systems*, vol. 53, no. 6, pp. 2987–2997, Dec. 2017.

[13] L. Daniel, S. Hristov, X. Lyu, A. G. Stove, M. Cherniakov, and M. Gashinova, 'Design and Validation of a Passive Radar Concept for Ship Detection Using Communication Satellite

Signals', *IEEE Transactions on Aerospace and Electronic Systems*, vol. 53, no. 6, pp. 3115–3134, Dec. 2017.

[14] S. Hristov *et al.*, 'Ship Detection Using Inmarsat BGAN Signals', in *International Conference on Radar Systems (Radar 2017)*, Belfast, UK, 2017.

[15] SpaceX Exploration Technologies Corp., 'SpaceX Non-Geostationary Satellite System - SATLOA2016111500118 - Schedule S Tech Report', SpaceX Exploration Technologies Corp., Schedule S Tech Report SATLOA2016111500118, Apr. 2016.